applied optics

Effective light absorption and its enhancement factor for silicon nanowire-based solar cell

ZHIQIANG DUAN,[1,2] MEICHENG LI,[2,*] TREVOR MWENYA,[2] PENGFEI FU,[2] YINGFENG LI,[2] AND DANDAN SONG[2]

[1]School of Mathematical and Physical Science, North China Electric Power University, Beijing 102206, China
[2]State Key Laboratory of Alternate Electrical Power System with Renewable Energy Sources, School of Renewable Energy, North China Electric Power University, Beijing 102206, China
*Corresponding author: mcli@ncepu.edu.cn

Received 12 October 2015; revised 22 November 2015; accepted 26 November 2015; posted 30 November 2015 (Doc. ID 251739); published 22 December 2015

Although nanowire (NW) antireflection coating can enhance light trapping capability, which is generally used in crystal silicon (CS) based solar cells, whether it can improve light absorption in the CS body depends on the NW geometrical shape and their geometrical parameters. In order to conveniently compare with the bare silicon, two enhancement factors E_T and E_A are defined and introduced to quantitatively evaluate the efficient light trapping capability of NW antireflective layer and the effective light absorption capability of CS body. Five different shapes (cylindrical, truncated conical, convex conical, conical, and concave conical) of silicon NW arrays arranged in a square are studied, and the theoretical results indicate that excellent light trapping does not mean more light can be absorbed in the CS body. The convex conical NW has the best light trapping, but the concave conical NW has the best effective light absorption. Furthermore, if the cross section of silicon NW is changed into a square, both light trapping and effective light absorption are enhanced, and the Eiffel Tower shaped NW arrays have optimal effective light absorption.

OCIS codes: (310.1210) Antireflection coatings; (080.2740) Geometric optical design; (160.4236) Nanomaterials; (350.6050) Solar energy.

http://dx.doi.org/10.1364/AO.55.000117

1. INTRODUCTION

Nanowire (NW) antireflective coating has a significant effect in reducing the reflection of light; thus, it is especially important and widely used to improve the light trapping capability in the field of crystal silicon (CS) solar cells [1,2]. Several studies have reported that optical absorption performance of NW solar cells is greatly influenced by the NW geometric parameters, such as the NW diameter, length, arrays density, volume filling ratio, etc. [3–6]. The optimal optical properties of NW solar cells can be obtained by reasonably modulating these parameters. Most of the studies have considered the NW antireflection coating and CS substrate as a whole and mainly focus on how to minimize the light reflection (R) and transmission (T) to increase the light absorption (A) by $A = 1 - R - T$. There is no doubt that the light trapping performance of CS solar cells is significantly enhanced after etching a NW antireflection layer, but it is often to neglect the difference of light absorption distribution between the NW antireflection layer (A_{NW}) and CS body (A_{Si}) where $A = A_{\mathrm{NW}} + A_{\mathrm{Si}}$, as shown in Fig. 1(a).

In this paper, compared with the naked CS, the enhancement factor of efficient light trapping E_T and effective light absorption E_A are defined as follows:

$$E_T = \frac{\mathrm{NAP}_{\mathrm{total}} - \mathrm{NAP}_{n\mathrm{Si}}}{\mathrm{NAP}_{n\mathrm{Si}}}, \tag{1}$$

$$E_A = \frac{\mathrm{NAP}_{\mathrm{Si}} - \mathrm{NAP}_{n\mathrm{Si}}}{\mathrm{NAP}_{n\mathrm{Si}}}, \tag{2}$$

where

$$\mathrm{NAP}_{\mathrm{total}} = \int A(\lambda)F(\lambda)\lambda/(h_0 c_0)\mathrm{d}\lambda, \tag{3}$$

$$\mathrm{NAP}_{\mathrm{Si}} = \int A_{\mathrm{Si}}(\lambda)F(\lambda)\lambda/(h_0 c_0)\mathrm{d}\lambda, \tag{4}$$

$$\mathrm{NAP}_{n\mathrm{Si}} = \int A_{n\mathrm{Si}}(\lambda)F(\lambda)\lambda/(h_0 c_0)\mathrm{d}\lambda. \tag{5}$$

$\mathrm{NAP}_{\mathrm{total}}$ is the total number of absorbed photons (each absorbed photon with energy greater than the bandgap produces one and only one electron-hole pair) in the whole body, including the CS body and the NW antireflective coating. $\mathrm{NAP}_{\mathrm{Si}}$ represents the number of absorbed photons in the CS body itself, which is a part of the whole, and $\mathrm{NAP}_{n\mathrm{Si}}$ means the number of

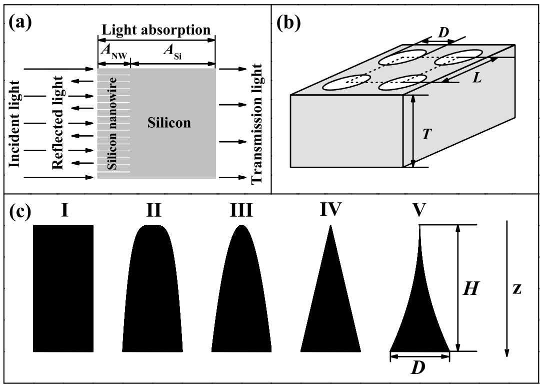

Fig. 1. (a) Distribution of light absorption (A_{NW} and A_{Si} are light absorption of antireflection layer and CS, respectively). (b) Structure diagram of NW arrays (D is the NW diameter, L is the period length, and T is the thickness of CS). (c) Shapes of NW (I, cylindrical, $m = 0$; II, parabolic truncated conical, $m = 0.50$; III, convex conical, $m = 1.0$; IV, conical, $m = 2.0$; V, concave conical, $m = 4.0$).

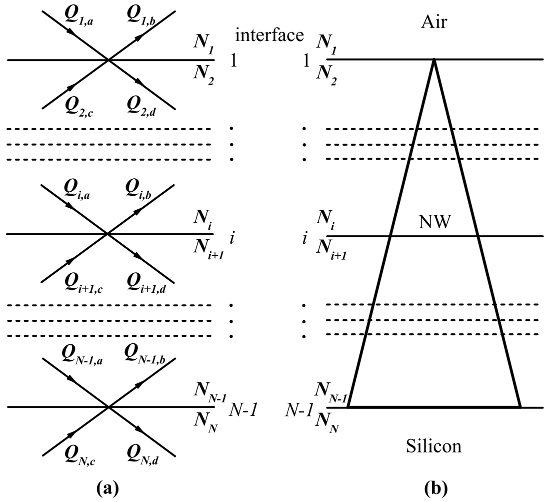

Fig. 2. (a) Schematic multilayer structure, with numbering convention of interfaces ($1, \ldots, i, \ldots, N-1$), refractive index ($N_1, \ldots, N_i, \ldots, N_N$), and energy fluxes ($Q_{i,a}, Q_{i,b}, Q_{i+1,c}, Q_{i+1,d}, \ldots$). (b) Schematic representation of silicon NW and effective multilayer structure.

absorbed photons of the naked CS. A, A_{NW}, and A_{Si} and their respective parts in light absorption are shown in Fig. 1(a). $F(\lambda)$ is the distribution of solar radiation spectral intensity on the Earth's surface under AM1.5 spectrum. λ is the wavelength of incident light, h_0 and c_0 are Planck constant and speed of light in vacuum, respectively. As shown in Fig. 1(b), the CS body with an antireflection layer of tapered silicon NW arrays arranged in a square is taken as an example. The cross section of NW is first considered a circle, and its contour shape is described by using a super-parabola profile function, i.e., Eq. (6):

$$r = (L/2)(z/H)^{m/2}, \qquad L = (1/\rho)^{1/2}, \tag{6}$$

where r is the NW radius, H is the NW length, L is the array's period length, ρ is the NW array's density. The thickness of CS is 100 μm, and the z axis is perpendicular to the CS surface. The top of the NW is at $z = 0$ and the bottom at $z = H$. When $m = 0$, the NW shape is cylindrical; for $m < 2$ or $m > 2$, the NW has a convex or concave shape, and, when $m = 2$, the NW has a conical shape. It is convenient to use the expression to depict different types of shapes by only changing the value of the parameter m, as shown in Fig. 1(c).

2. SIMULATION METHODS

The net radiation method (NRM) [7,8] and effective medium approximation (EMA) [9,10] are used in our theoretical calculations. NRM is suitable for illustrating the transmission, absorption, and reflection characteristics of a multilayer medium for incident radiation based on its good matching between simulation and experimental results. As shown in Fig. 2(a), a system of N layers, a, c and b, d represent the incoming and outgoing light radiation, respectively. The interfaces are labeled $i = 1, \ldots, N-1$, where i is the total number of interfaces, and N_i is the refractive index of the ith medium. The relations between the outgoing and incoming energy fluxes (Q) at each interface can be expressed in terms of the reflection at the interface and the transmission passing through the medium. For every interface i, there are four equations:

$$\begin{cases} Q_{i,a} = \tau_i Q_{i,d} \\ Q_{i,b} = r_{i,i+1} Q_{i,a} + t_{i+1,i} Q_{i+1,c} \\ Q_{i+1,c} = \tau_{i+1} Q_{i+1,b} \\ Q_{i+1,d} = t_{i,i+1} Q_{i,a} + r_{i+1,i} Q_{i+1,c} \end{cases}. \tag{7}$$

The reflectivity and transmittivity at each of the interface is $r_{i,i+1}$ and $t_{i,i+1}$ (subscripts indicate energy fluxes transferring from layer i to layer $i+1$), which are determined using Fresnel's laws, $r_{i,i+1} + t_{i,i+1} = 1$, and vice versa, $r_{i+1,i} + t_{i+1,i} = 1$. τ_i is the absorption attenuation rate of layer i, defined by

$$\tau_i = \exp(-\alpha d_i / \cos \varphi), \tag{8}$$

where $\alpha = 4\pi k/\lambda$ is the absorption coefficient and $d_i / \cos \varphi$ is the distance traveled through the layer of thickness d_i with propagation angle φ. k is the imaginary part of the complex refractive index $N_{nk} = n - ik$. Both the real refractive index n and the extinction coefficient k are functions of λ. Assuming the incident energy flux $Q_{1,a} = 1$ and $Q_{N,c} = 0$, then, for each layer, the spectral reflectance $R_{i,i+1} = Q_{i,b}$, transmittance $T_{i,i+1} = Q_{i+1,d}$ and absorptance $A_{i,i+1} = Q_{i,a} - R_{i,i+1} - T_{i,i+1}$ can be worked out.

The effective multilayer structure of silicon NW is shown in Fig. 2(b), and the refractive indices of different NW layers can be solved by the EMA formula:

$$\frac{f_1(N_{Si}^2 - N_{Eff}^2)}{(N_{Si}^2 + 2N_{Eff}^2)} + \frac{f_2(N_{Air}^2 - N_{Eff}^2)}{(N_{Air}^2 + 2N_{Eff}^2)} = 0, \tag{9}$$

where f_1 and f_2 are the ratio of volume filling of silicon NW and air, respectively, and $f_1 + f_2 = 1$. N_{Si}, N_{Air}, and N_{Eff} are the complex refractive indices of CS, air, and the interlayer of NW, respectively.

Before starting the calculations, related parameters are assumed as follows: the NW array's density ρ is set as 100 μm^{-2}, so the array's period length $L = 100$ nm; the maximum value of NW bottom diameter $D = L = 100$ nm and the NW length $H = 1.0$ μm; the thickness of CS substrate $T = 100$ μm; the layer thickness $d_i = 10$ nm, and it is also the minimum step in calculating.

3. RESULTS

First, taking the NW antireflection layer and the CS body as a whole, the effect of different shapes of NW arrays on optical performance is studied. As shown in Fig. 3, compared with the naked CS, there is a better light trapping effect with the NW antireflection coating than without it. Among the five NW shapes, the shape of "I" (the cylindrical NW) has the weakest ability to lower the light reflection, and the other tapered NW has better antireflection capability, as shown in Figs. 3(a) and 3(b). This means that the bigger top cross-sectional area will block the light incidence [3,11]. Furthermore, the shape of "III" (the convex conical NW) has better antireflection and absorption capability than others, as seen in Figs. 3(d) and 3(e). For the whole structure, the light absorption is enhanced for wavelengths less than 1.17 μm; for the longer wavelength region, the more the light antireflection, the more the light transmission because the light in this wavelength range cannot be absorbed by CS, as shown in Figs. 3(c) and 3(f). For the five NW shapes, if taken as a whole, the ranking order of light trapping performance is III > IV > II > V > I. This result is consistent with previous research findings and the conclusion that the tapered Si NW has strong light trapping ability [12,13].

The NW antireflection coating can enhance light trapping characteristics, but, in the meantime, the increased surface recombination losses represent a handicap for high-efficiency solar cells [11]. Therefore, our concern is about how to increase the amount of photons that be absorbed after the surface texturization. In our research, the absorbed photons are divided into two parts: Φ_{NW} and Φ_{Si}, which are absorptivity of photon flux (APF) of NW antireflection coating and CS body, respectively. Here, for comparison's sake, it is assumed that the photons, which are absorbed by NW antireflection coating, are used to compensate for surface recombination losses and that the photons, which are absorbed by the CS body, can be efficiently utilized and completely converted into electron-hole pairs. Thus, for A_{Si}, a higher value is better, and, for A_{NW}, a lower value is better. The differences of light absorptivity and APF between the NW antireflection layer and CS body are shown in Fig. 4. For shape of "I," as a whole, although there is a little contribution to the light trapping effect than that of naked silicon, which can be seen in Fig. 3(a), there is little enhancement in improving the light absorption in the CS body and even worse than naked CS, as seen in Figs. 4(b) and 4(d). The main cause of this situation is that the NW antireflection layer has absorbed part of the photons. For other shapes, obviously, the NW antireflection layer basically absorbs part of the high-energy photons. The light absorptivity and APF show a decreasing trend with decrease in NW volume, and the absorption peak declines and appears to shift to the shorter wavelength, as shown in Figs. 4(a) and 4(c). Other high-energy photons, which are not absorbed by the NW antireflection layer, enter the CS body and are absorbed by it, as shown in Figs. 4(b) and 4(d). In this sense, the light trapping ability of NW antireflection coating is further enhanced, and the NW has a similar effect on the antenna [14,15].

As previously mentioned, our concern is about how to increase the amount of photons that can be absorbed by the CS body compared with the naked CS, and this is what the NW antireflection layer really does. To make the difference between them more intuitionistic, a 3D illustration is necessary.

There is an important parameter, the ratio of the NW diameter to the array period length, i.e., D/L. This parameter is closely related to the effective refractive index of the NW antireflection layer, which affects the change of photon absorption. variations of the enhanced factors E_T and E_A under different geometric parameters are studied and shown in Fig. 5. First, for

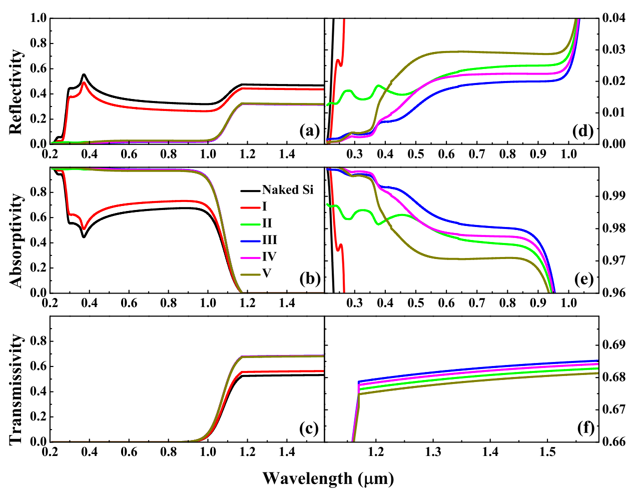

Fig. 3. (a)–(c) Calculated reflectivity, absorptivity, and transmissivity of the CS substrate covered with NW antireflection coating compared with the naked CS. (The five simulation shapes: I, cylindrical; II, parabolic truncated conical; III, convex conical; IV, conical; V, concave conical, respectively.) Right inset (d)–(f): partially enlarged corresponding to the left.

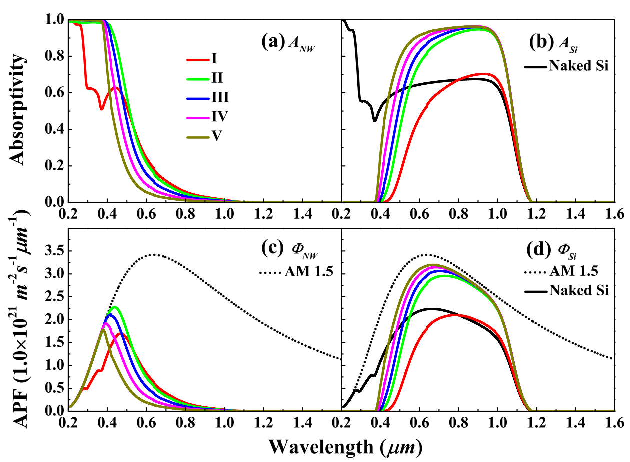

Fig. 4. (a) and (c) Light absorptivity A_{NW} and absorptivity of photon flux (APF) Φ_{NW} of silicon NW coating, respectively. (b) and (d) Light absorptivity A_{Si} and absorptivity of photon flux (APF) Φ_{Si} of CS body compared with the naked silicon under AM, respectively. 1.5 spectrum.

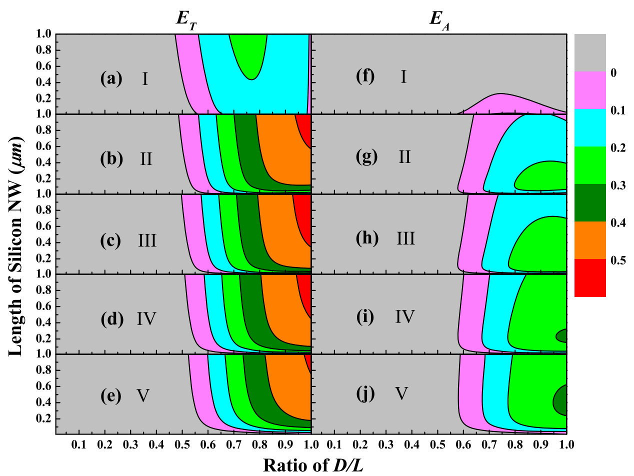

Fig. 5. (a)–(e) Contour map of enhancement factor E_T under different values of H and D/L, which are corresponding to NW shape of "I," "II," "III," "IV," and "V" having the circle cross section. (f)–(j) Contour maps of enhancement factor E_A under different values of H and D/L, which are corresponding to NW shape of "I," "II," "III," "IV," and "V" having the circle cross section.

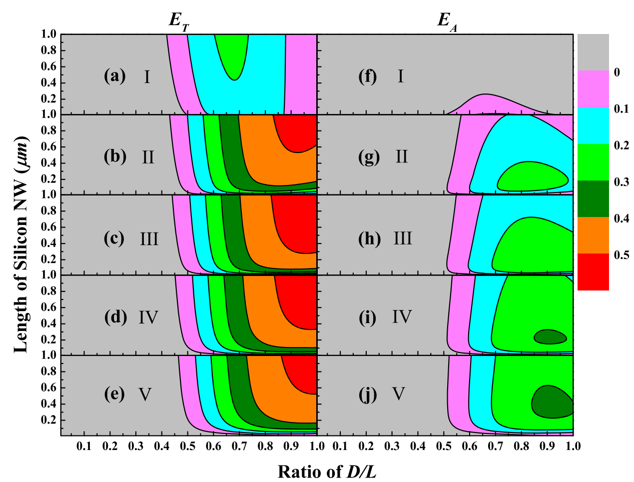

Fig. 6. (a)–(e) Contour map of enhancement factor E_T under different values of H and D/L, which are corresponding to NW shape of "I," "II," "III," "IV," and "V" having the square cross section. (f)–(j) Contour map of enhancement factor E_A under different values of H and D/L, which are corresponding to NW shape of "I," "II," "III," "IV," and "V" having the square cross section.

the cylindrical NW shown in Figs. 5(a) and 5(f), only when the value of D/L is in the range of 0.69–0.82 and H is greater than 0.440 μm, there is improved best light trapping property and E_T is the biggest and near 0.21, which is consistent with the present results [3]. However, under these conditions, E_A is less than zero and cannot compete with the naked CS. It means the NW alone absorbs all of the photons, instead of being absorbed by the CS body. For E_A, its maximum value is near 0.13 only when the value of D/L is in the range of 0.70–0.89, H is less than 0.300 μm, and, under the same conditions, E_T is only about 0.17, less than 0.21. This implies that better light trapping does not translate into better light absorption. Next, for other NW shapes, values of E_T are greater than that for the shape of "I" under the same conditions, and, for the shape of "III," it can reach the biggest value of 0.52. Among them, E_T of shape of "III" has a little advantage as compared with others shown as the larger area, where E_T is greater than 0.5, as shown in Fig. 5(c). It reflects the parabolic contours of NW having least resistance to the flow of photons and improves the light absorption. Quite unexpectedly, E_A of shape of "III" is not the largest, while E_A of shape of "V" is the largest of about 0.31, as shown as the larger area, where E_A is greater than 0.3, as shown in Fig. 5(j). Through the analysis, it can be concluded that photon absorption is not only related to the NW volume but also on the NW shape, which mainly depends on the small tip and the larger base [13,16]. The number of photons, which should be absorbed by the NW antireflection layer, is reduced due to the unique NW morphology, so there are more photons penetrating through the NW antireflection layer and then absorbed by the CS body.

Several conclusions can be reached through analysis of Fig. 5. First, the tapered NW (shape of "II," "III," "IV," and "V") has better optical properties than the cylindrical NW (shape of "I"), no matter for light trapping or effective light absorption. Second, with longer NW, there is better light trapping ability [17,18] but poor effective light absorption. Third, for the tapered NW, the larger the ratio of D/L and the closer it is to equal 1, the better are the light trapping and effective light absorption. The third conclusion implies that the best arrangement for the NW arrays is that the NW should be arranged closely and without gaps. Therefore, the square cross-section NW arrays are considered next.

With the NW array density unchanged, the performances of light trapping and effective light absorption of square cross-section NW are studied and are shown in Fig. 6. Compared with the circle cross-section NW shown in Fig. 5, there is a tendency of blueshift for both E_T and E_A corresponding to the maximum value of their optimal properties. Under the same conditions, the square cross-section NW arrays have the larger values of E_T and E_A than does the circle cross-section NW. Among the five shapes of NW, in the same way, the shape of "V," whose apparent shape is like the Eiffel Tower's, has the most obvious advantage.

4. CONCLUSIONS

We have investigated the optical absorption of silicon NW-based solar cells, which can be divided into two parts: the light absorption of the surface NW arrays; the CS body. The main function of the antireflection layer is to reduce light reflection and increase light transmission; the CS substrate is the main place where photons are absorbed and converted. Computer simulations demonstrate that the NW arrays can increase the optical absorption, and it depends on not only the NW diameter, length, and volume filling ratio but also on the shape of the cross section. By studying the circular and square cross-section NW, based on the definition of enhancement factors E_T and E_A, we found that silicon NW, which is shaped like the Eiffel Tower, has the largest amount of photon absorption even when its light trapping capability is not the best.

Therefore, the enhancement factor E_A should be considered as the key index in the design of a light-trapping structure.

Funding. Fundamental Research Funds for the Central Universities (11ZG02); National Natural Science Foundation of China (NSFC) (50972032, 51172069, 51372082, 91333122); Ph.D. Programs Foundation of Ministry of Education of China (20110036110006, 20120036120006, 20130036110012).

REFERENCES

1. Z. Xu, J. Jiang, and G. L. Liu, "Lithography-free sub-100 nm nanocone array antireflection layer for low-cost silicon solar cell," Appl. Opt. **51**, 4430–4435 (2012).
2. M. Abouda Lachiheb, M. A. Zrir, N. Nafie, O. Abbes, J. Yakoubi, and M. Bouaïcha, "Investigation of the effectiveness of SiNW used as an antireflective layer in solar cells," Sol. Energy **110**, 673–683 (2014).
3. Z. Duan, M. Li, T. Mwenya, F. Bai, Y. Li, and D. Song, "Geometric parameter optimization to minimize the light-reflection losses of regular vertical silicon nanorod arrays used for solar cells," Phys. Status Solidi A **211**, 2527–2531 (2014).
4. J.-Y. Jung, H.-D. Um, S.-W. Jee, K.-T. Park, J. H. Bang, and J.-H. Lee, "Optimal design for antireflective Si nanowire solar cells," Sol. Energy Mater. Sol. Cells **112**, 84–90 (2013).
5. K. Zhou, X. Li, S. Liu, and J.-H. Lee, "Geometric dependence of antireflective nanocone arrays towards ultrathin crystalline silicon solar cells," Nanotechnology **25**, 415401 (2014).
6. Y. Zhan, X. Li, S. Wu, K. Li, Z. Yang, and A. Shang, "Enhanced photoabsorption in front-tapered single-nanowire solar cells," Opt. Lett. **39**, 5756–5759 (2014).
7. R. Santbergen and R. J. C. van Zolingen, "The absorption factor of crystalline silicon PV cells: a numerical and experimental study," Sol. Energy Mater. Sol. Cells **92**, 432–444 (2008).
8. R. Santbergen, A. H. M. Smets, and M. Zeman, "Optical model for multilayer structures with coherent, partly coherent and incoherent layers," Opt. Express **21**, A262–A267 (2013).
9. A. Najar, J. Charrier, P. Pirasteh, and R. Sougrat, "Ultra-low reflection porous silicon nanowires for solar cell applications," Opt. Express **20**, 16861–16870 (2012).
10. H. Wang, X. Liu, L. Wang, and Z. Zhang, "Anisotropic optical properties of silicon nanowire arrays based on the effective medium approximation," Int. J. Therm. Sci. **65**, 62–69 (2013).
11. F. Xiu, H. Lin, M. Fang, G. Dong, S. Yip, and J. C. Ho, "Fabrication and enhanced light-trapping properties of three-dimensional silicon nanostructures for photovoltaic applications," Pure Appl. Chem. **86**, 557–573 (2014).
12. J.-Y. Jung, Z. Guo, S.-W. Jee, H.-D. Um, K.-T. Park, and J.-H. Lee, "A strong antireflective solar cell prepared by tapering silicon nanowires," Opt. Express **18**, A286–A292 (2010).
13. B. Wang, E. Stevens, and P. W. Leu, "Strong broadband absorption in GaAs nanocone and nanowire arrays for solar cells," Opt. Express **22**, A386–A395 (2014).
14. E. Robak, B. Grzeskiewicz, and M. Kotkowiak, "Absorption enhancement in silicon nanowire-optical nanoantenna system for photovoltaic applications," Opt. Mater. **37**, 104–109 (2014).
15. Y. Li, M. Li, P. Fu, R. Li, D. Song, C. Shen, and Y. Zhao, "A comparison of light-harvesting performance of silicon nanocones and nanowires for radial-junction solar cells," Sci. Rep. **5**, 11532 (2015).
16. B. Wang and P. W. Leu, "Enhanced absorption in silicon nanocone arrays for photovoltaics," Nanotechnology **23**, 194003 (2012).
17. R. Y. Zhang, B. Shao, J. R. Dong, J. C. Zhang, and H. Yang, "Absorption enhancement analysis of crystalline Si thin film solar cells based on broadband antireflection nanocone grating," J. Appl. Phys. **110**, 113105 (2011).
18. V. Trinh Pham, M. Dutta, H. Bui, and N. Fukata, "Effect of nanowire length on the performance of silicon nanowires based solar cell," Adv. Nat. Sci. **5**, 045014 (2014).